ELSEVIER

Polymer 42 (2001) 3171–3182

polymer

www.elsevier.nl/locate/polymer

Modeling of non-isothermal crystallization kinetics of isotactic polypropylene

Y. Mubarak, E.M.A. Harkin-Jones*, P.J. Martin, M. Ahmad

Polymer Processing Research Centre, The Queen's University of Belfast, Ashby Building, Stranmillis Road, Belfast BT9 5AH, UK

Received 21 February 2000; received in revised form 4 July 2000; accepted 11 August 2000

Abstract

Isothermal and non-isothermal melt crystallization kinetics of isotactic polypropylene (iPP) were investigated via differential scanning calorimetry (DSC). Isothermal melt crystallization kinetics were analyzed using the Avrami equation. An Avrami exponent close to three was obtained for iPP, which implies growth of three-dimensional spherulitic superstructures following heterogeneous nucleation. Non-isothermal crystallization kinetics data obtained from DSC in conjunction with a non-linear regression method were employed to estimate the kinetic parameters of mathematical models describing the non-isothermal crystallization of iPP. The results suggest that the available mathematical models are not successful in describing the non-isothermal crystallization of iPP over a wide range of cooling rates. It was found that the non-isothermal crystallization kinetics of iPP, over a wide range of cooling rates, could best be described by modifying the Ozawa model to include induction times.

Keywords: Polypropylene; Non-isothermal crystallization kinetics; Differential scanning calorimetry

1. Introduction

Isotactic polypropylene (iPP) is a semi-crystalline polymer of considerable commercial importance; it has low density and price, good toughness, excellent water and chemical resistance, and ease of processability.

A semi-crystalline polymer such as polypropylene when cooled from the melt either under isothermal or non-isothermal conditions will form a crystalline structure. Two competitive effects influence the crystallization behavior; cooling rate and crystallization growth rate. The resulting microstructure has a significant effect on the ultimate properties of the product such as toughness, elasticity, transparency, or permeability. In turn, the microstructure of the material is determined by the thermochemical history that the material experiences during processing.

Practical processes usually proceed under non-isothermal crystallization conditions. In order to search for the optimum conditions in an industrial process and to obtain products with better properties, it is necessary to have quantitative evaluations of the non-isothermal crystallization process.

The objective of this study was to investigate the validity of published mathematical models for the non-isothermal crystallization kinetics of iPP as it crystallizes from the melt over a wide range of cooling rates.

2. Theoretical background

Several models have been proposed for the theoretical treatment of isothermal crystallization kinetics. Avrami [1] proposed an isothermal model which has been used universally to describe polymer crystallization kinetics. The change in crystallinity with time can be readily expressed as:

$$\theta(t) = 1 - \exp(-k(T)t^n) \tag{1}$$

where θ is the relative crystallinity at time t; n, the Avrami index (crystal geometry information); T, the crystallization temperature; and k, the isothermal crystallization rate constant containing the nucleation and growth rates. Eq. (1) can be transformed into logarithmic form.

$$\ln[-\ln(1 - \theta(t))] = n \ln(t) + \ln(k) \tag{2}$$

Applying Avrami theory, a plot of $\ln[-\ln(1 - \theta(t))]$ versus $\ln(t)$ should yield a straight line with slope n and intercept k.

In many cases, isothermal models are experimentally accessible only over a narrow temperature range that is often well above that where crystallization occurs in processing [2]. Non-isothermal modeling is therefore essential for

* Corresponding author. Tel.: +44-28-90274490.
E-mail address: e.harkinJones@qub.ac.uk (E.M.A. Harkin-Jones).

0032-3861/01/$ - see front matter
PII: S0032-3861(00)00606-6

the understanding of the crystallization behavior of a semi-crystalline polymer. Various modifications of the Avrami equation have been made in order to model non-isothermal crystallization kinetics. These models will be described below.

Nakamura et al. [3] have extended the Avrami equation to describe the transformation process occurring in non-isothermal crystallization on the basis of isokinetic conditions. The number of activated nuclei is considered to be independent of temperature and the nucleation rate and the growth rates have the same time dependence.

$$\theta(t) = 1 - \exp\left[-\left(\int_0^t K(T)\,\mathrm{d}t\right)^n\right] \tag{3}$$

where $K(T)$ is related to the crystallization rate constant of the isothermal crystallization $k(T)$ through the relation: $K(T) = k(T)^{1/n}$. This model was only tested against experimental data obtained within a very narrow range of temperatures (from 127 to 117°C) at a maximum cooling rate of less than 0.5°C/min.

Kamal and Chu [4] proposed a modified Avrami equation in order to obtain a more extensive and reliable characterization of isothermal crystallization kinetics. Based on the assumption that non-isothermal crystallization may be treated as a sequence of isothermal crystallization steps, and neglecting secondary crystallization, a procedure was recommended and employed to predict non-isothermal crystallization behavior for high-density polyethylene (HDPE) resins over a range of cooling rates from 2.5 to 20°C/min using the following equation:

$$\theta(t) = 1 - \exp\left[-\int_0^t k(T) n t^{n-1}\,\mathrm{d}t\right] \tag{4}$$

In comparison with the experimental non-isothermal crystallization data, model predictions were within ±15%.

Taking into account the effects of temperature lag between the sample and the differential scanning calorimetry (DSC) furnace and non-isothermal induction times which are obtained from isothermal induction times, Chan and Isayev [5] analyzed the non-isothermal crystallization data for poly(ethylene terephthalate) (PET) over a range of cooling rates from 2 to 40°C/min using the differential form of the Nakamura equation.

$$\frac{\mathrm{d}\theta}{\mathrm{d}t} = nK(T)(1-\theta)[-\ln(1-\theta)]^{(n-1)/n} \tag{5a}$$

$$K(T) = k(T)^{1/n} = (\ln 2)^{1/n}(1/t_{1/2}) \tag{5b}$$

$$(1/t_{1/2}) = (1/t_{1/2})_0 \exp\left(\frac{-U^*}{\mathrm{R}(T-T_\infty)}\right)\exp\left(\frac{-K_\mathrm{g}}{T\Delta Tf}\right) \tag{5c}$$

where T is the crystallization temperature; $t_{1/2}$, the time taken for half of the crystallization to develop; $(1/t_{1/2})_0$, a pre-exponential factor that includes all terms independent of temperature; R, the universal gas constant; $\Delta T = T_\mathrm{m}^0 - T$, the supercooling; T_m^0, the equilibrium melting temperature; $f = 2T/(T + T_\mathrm{m}^0)$, a correction factor accounting for the reduction in the latent heat of fusion as the temperature is decreased; $T_\infty = T_\mathrm{g} - 30$ K, the temperature below which transport ceases; T_g, the glass-transition temperature; U^*, the activation energy for segmental jump rate in polymers; and K_g, the nucleation exponent.

They calculated the relative crystallinity developed during non-isothermal crystallization under various constant cooling/heating rates with and without the inclusion of induction time. The results with the incorporation of induction time show generally good agreement between the experimental data and the model predictions.

Dietz [6] noted that none of the available models account for the effects of secondary crystallization. Therefore the author introduced an additional term into the rate of crystallization equation in order to describe the transition from spherulitic growth to post crystallization. The following crystallization rate equation was proposed to account for slower secondary crystallization:

$$\frac{\mathrm{d}\theta}{\mathrm{d}t} = nk(T)(1-\theta)t^{n-1}\exp\left[\frac{-a\theta}{1-\theta}\right] \tag{6}$$

where parameter a lies between zero and one. The Dietz model is in fact a modification of a differential form of the Kamal and Chu model and introduces an additional parameter that must be evaluated.

Patel and Spruiell [2] presented an analysis of available methods of dealing with polymer crystallization for process modeling. Problems encountered in using isothermal data to predict non-isothermal results are discussed and illustrated using non-isothermal experimental data for nylon 6 collected over a range of cooling rates from 2 to 40°C/min. It was concluded that none of the available models is entirely satisfactory in predicting non-isothermal crystallization based on isothermal data. These authors used a non-linear regression method to fit their non-isothermal crystallization data using a simplified differential Nakamura model. By letting $Y = \ln(1/(1-\theta))$, the non-isothermal crystallization rate equation was written as follows:

$$\frac{\mathrm{d}Y}{\mathrm{d}t} = nK(T)(Y)^{(n-1)/n} \tag{7a}$$

$$K(T) = k(T)^{1/n} = C_1 \exp\left[\frac{-U^*}{\mathrm{R}(T-T_\infty)}\right]\exp\left[\frac{-C_2}{T\Delta Tf}\right] \tag{7b}$$

$$C_1 = (\ln 2)^{1/n}(1/t_{1/2})_0 \tag{7c}$$

where C_1 and C_2 are the parameters of the crystallization rate equation. Keeping $n = 2$, the non-isothermal data was fitted with various pairs of values of C_1 and C_2 (parameters of the model). For constant values of C_2, the data for each cooling rate was fitted individually to obtain the C_1 value. Different values for C_1 were obtained for different cooling

rates. Using the average value of C_1, predictions according to the simplified differential Nakamura model were found to match the experimental data in the range of cooling rates from 2 to 40°C/min.

Ding and Spruiell [7] reported that none of the kinetic models could fit or predict non-isothermal experimental data in an entirely satisfactory manner, even under low cooling rate conditions. Further, most of the approaches are modification or extension of the well-established Avrami equation, which is commonly used to interpret isothermal crystallization kinetics. Therefore, a power law nucleation rate function was proposed to describe the way in which nucleation rate varies with time during the non-isothermal or isothermal crystallization of polymers. The modified Avrami equation was written as follows:

$$\theta = 1 - \exp[-k' t^{n^*}] \tag{8a}$$

where the crystallization rate constant, k', and Avrami index n^* are given by:

$$k' = N_c n' A_g G^{n'} B(m+2, n') \tag{8b}$$

$$n^* = n' + m + 1 \tag{8c}$$

$$B(m+2, n') = \int_0^1 q^{m+2-1}(1-q)^{n'-1}\,dq \tag{8d}$$

with n', the geometric index, determined by the shape of the growing spherulites; N_c, the nucleation rate constant; m, the nucleation index; A_g, a constant which depends on the geometric shape of the transformed entities; $B(m+2, n')$, defined to be the B-function; and G, the growth rate. This modified Avrami equation was found to be suitable for kinetics analysis for the data obtained from non-isothermal crystallization at rapid cooling rates. The model was applied to analyze non-isothermal crystallization data of iPP obtained at various cooling rates (≤2500°C/min). The Avrami index (n^*) and crystallization rate constant (k') were obtained from the linear section, corresponding to primary crystallization, of the Avrami plot (Eq. (2)) for non-isothermal crystallization data. Fitting the proposed model (Eq. (8)) to the data for non-isothermal crystallization showed that the model describes the experimental data well in the range of relative crystallinities up to about 80% which is the stage before the occurrence of impingement.

Following the same approach and applying the Avrami theory (Eq. (2)), non-linear curves were obtained for the non-isothermal crystallization data for cooling rates from 1 to 100°C/min used in the present study. Hence, it was not possible to obtain reasonable values for the Avrami index (n^*) and crystallization rate constant (k') from these curves.

Kim et al. [8] studied the nucleation effects of two sorbital derivatives on the crystallization of iPP by means of DSC. A non-isothermal crystallization kinetic equation was employed to analyze the crystallization characteristics of iPP with and without nucleating agents. The non-isothermal crystallization kinetic equation used was proposed by Tobin and based upon the theory of transition kinetics with growth site impingement, and its final expression was derived by Choe and Lee [9]. The equation is a linear combination of two terms concerning the growth processes initiated by heterogeneous and homogenous nucleation, which are considered to be competing with each other in the dynamic crystallization process, and is written as follows:

$$\dot{\alpha}(t) = \dot{\alpha}_1(t) + \dot{\alpha}_2(t) \tag{9a}$$

$$\dot{\alpha}_1(t) = k_1 \exp\left(\frac{-3E_d}{RT}\right) \exp\left(\frac{-3\psi_1 T_m^0}{T(T_m^0 - T)}\right) t^2 [1-\alpha(t)]^2 \tag{9b}$$

$$\dot{\alpha}_2(t) = k_2 \exp\left(\frac{-4E_d}{RT}\right) \exp\left(\frac{-(3\psi_1 + \psi_2)T_m^0}{T(T_m^0 - T)}\right) [1 - \alpha(t)]^2 \int_0^t (t-\omega)^2 [1-\alpha(\omega)]\,d\omega \tag{9c}$$

where $\dot{\alpha}(t)$ is the overall crystallization rate at time t; $\dot{\alpha}_1(t)$, the crystallization rate contributed by the growth process initiated by heterogeneous nucleation; $\dot{\alpha}_2(t)$, the crystallization rate contributed by the growth process initiated by homogeneous nucleation; k_1, the rate constant for $\dot{\alpha}_1(t)$; E_d, the diffusional activation energy of crystallizing segments across the phase boundary; ψ_1, a constant related to the free energy of formation of a critical nucleus on the growing crystal surface; k_2, the rate constant for $\dot{\alpha}_2(t)$; and ψ_2, a constant related to the free energy of formation of a growth embryo in the homogeneous nucleation process.

Applying Marquardt's [10] non-linear multivariable regression method and the fourth order Runge–Kutta integration technique to the data obtained from the dynamic DSC tests, the kinetic parameters in the model equation were determined. The authors concluded that non-isothermal crystallization kinetics analysis for the un-nucleated iPP at different cooling rates was possible by assuming a spherulite growth initiated simultaneously by heterogeneous and homogenous nucleation, and that the crystallization kinetics of the nucleated iPP could be described by the heterogeneous nucleation and growth process alone. Hammami and Mehrotra [11] re-examined the model proposed by Choe and Lee (Eq. (9)) and reported that the expression for the homogeneous nucleation rate was incorrectly written. The model also did not account for the expected change in heat of fusion at temperatures below the equilibrium melting point. Hence, the proposed model by Choe and Lee (Eq. (9)) will not be further pursued here. Hammami and Mehrotra reported the following corrections for

non-isothermal crystallization:

$$\dot{\alpha}_1(t) = k_1 \exp\left(\frac{-3E_d}{RT}\right)\exp\left(\frac{-3\psi_1 T_m^0}{fT(T_m^0 - T)}\right)t^2[1-\alpha(t)]^2 \tag{10a}$$

$$\dot{\alpha}_2(t) = k_2 \exp\left(\frac{-4E_d}{RT}\right)\exp\left(\frac{-\psi_2 (T_m^0)^2}{f^2 T(T_m^0 - T)} - \frac{3\psi_1 T_m^0}{fT(T_m^0 - T)}\right) \times [1-\alpha(t)]^2 \int_0^t (t-\omega)^2[1-\alpha(\omega)\,d\omega \tag{10b}$$

The authors did not test the corrected model to fit any non-isothermal crystallization data.

Note: in this present study, the corrected model (Eq. (9)) was examined to fit the non-isothermal crystallization data of iPP. The non-linear regression software used could not find any reasonable fit for the data, and so this model was not pursued any further.

In the parallel Avrami model of Velisaris and Seferis [12], the relative degree of crystallinity during isothermal crystallization at temperature T is written as:

$$\frac{X_{vc}}{X_{vc\infty}} = w_1[1-\exp(-k_1(T)t^{n_1})] + w_2[1-\exp(-k_2(T)t^{n_2})] \tag{11a}$$

with $w_1 + w_2 = 1$, $k_1(T)$ and $k_2(T)$ are the crystallization rate constants for the first and second terms, respectively; n_1 and n_2, the Avrami exponents; w_1 and w_2, the weight fractions; X_{vc}, the volume fraction crystallinity; and $X_{vc\infty}$, the equilibrium volume fraction crystallinity. This expression corresponds to the two different nucleation or growth processes occurring in parallel, with the relative importance of each manifested by the values of the weight factors, w_1 and w_2. To apply the model to non-isothermal crystallization, Velisaris and Seferis expressed a crystallization kinetics model in terms of a linear combination of two time-integral expressions in parallel having the following form:

$$\frac{X_{vc}}{X_{vc\infty}} = w_1[1-\exp(-\int_0^0 k_1(T)n_1 t^{n_1-1}\,dt)] + w_2[1-\exp(-\int_0^t k_2(T)n_2 t^{n_2-1}\,dt)] \tag{11b}$$

The validity of the dual mechanism crystallization model was proven in practice by predicting the non-isothermal crystallization kinetics of polyetheretherketone (PEEK) for samples crystallized at constant cooling rates from 10 to 60°C/min. In order to provide the best fit to the data, the authors selected $n_1 = 2.5$ and $n_2 = 1.5$ and based on the DSC melting point, two different melting temperatures (T_m^0) were used to calculate the degree of undercooling (ΔT) for the first and second terms. An equilibrium volume fraction crystallinity ($X_{vc\infty}$) value was selected from the literature. All other parameters were allowed to vary between the data sets, and all were fitted with a non-linear least-square modeling program. A good correspondence between the model and the experimental non-isothermal crystallization data was obtained.

Cebe [13] re-examined the parallel Avrami model proposed by Velisaris and Seferis (Eq. (11)) employing a non-linear least squares fitting routine to fit the data separately for non-isothermal cooling rates of 1, 5, and 10°C/min. The author reported that several revisions were necessary in order to correctly apply the model. The author found that the values of the parameters for the two processes did vary with different initial choices for n_1 and n_2.

Verhoyen et al. [14] developed a new isothermal crystallization model namely the consecutive Avrami model:

$$\frac{\alpha(t)}{\alpha_v^\infty} = w_1(1-\exp(-k_1(t-t_0^1)^{n_1})) + w_2(1-\exp(-k_2(t-t_0^2)^{n_2})) \tag{12}$$

and using the same approach as Nakamura they extended their consecutive model to non-isothermal processes and derived the following model:

$$\alpha_v(t) = \int_0^t \alpha_v^\infty w_1 \frac{\partial}{\partial\tau}\left(1-\exp\left(-\left[\int_{t_0^{1*}}^{\tau} \sqrt[k_1]{n_1}\,ds\right]^{n_1}\right)\right)d\tau + \int_0^t \alpha_v^\infty (1-w_1)\frac{\partial}{\partial\tau}\left(1-\exp\left(-\left[\int_{t_0^{2*}}^{\tau} \sqrt[k_2]{n_2}\,ds\right]^{n_2}\right)\right)d\tau \tag{13}$$

where α_v is the degree of crystallinity at time t; α_v^∞, the final degree of crystallinity; w_1 and w_2, weight factors; k_1 and k_2, the rate constants due to primary and secondary crystallization; n_1 and n_2, Avrami indices; t_0^1 and t_0^2, isothermal induction times; t_0^{1*} and t_0^{2*}, the non-isothermal induction times for the first and second mechanisms, respectively. This model, which takes into account ultimate crystallinity degree, induction time and secondary crystallization, was developed for PET and can be applied to other high T_g polymers. The parameters of this model were determined through isothermal crystallization kinetic experiments using DSC. From these parameters, interpolation functions were obtained which, when combined with the consecutive model (Eq. (12)), allow for the prediction of isothermal crystallization kinetics, and introducing the interpolation functions into the extended Nakamura model (Eq. (13)) allows for the prediction of non-isothermal crystallization kinetics.

To apply the consecutive model (Eq. (13)) to non-isothermal crystallization data, it is necessary to obtain the interpolation functions for α_v^∞, w_1, k_1, k_2, t_0^1, and t_0^2 as a function of T, T_m^0, and T_g. The data available in this study is not enough to build up the required interpolation functions to apply the model and the consecutive Avrami model will not therefore be examined.

Ozawa [15] derived a non-isothermal kinetics model for the process of nucleation and its growth by extending the

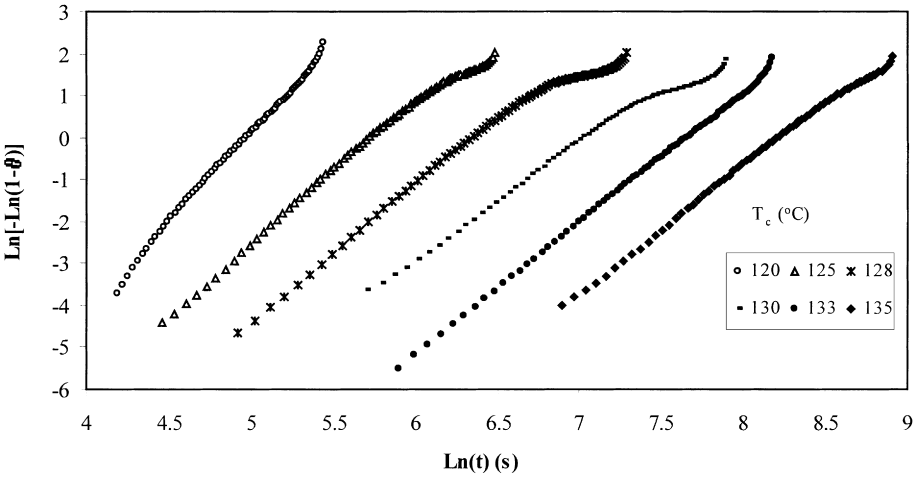

Fig. 1. Avrami plots of iPP at different constant temperatures.

Avrami equation. The kinetic analysis of the thermoanalytical data of the process was applied to DSC curves of crystallization obtained by cooling the melt at constant rates. The following equation was proposed:

$$\theta = 1 - \exp\left[\frac{-\chi(T)}{\lambda^n}\right] \tag{14}$$

where $\chi(T)$ is the cooling function for non-isothermal crystallization at temperature T and λ is the cooling rate. Ozawa's equation should find little application in process modeling because a constant cooling rate is assumed and values of relative crystallinities at a fixed temperature for different cooling rates are required. Furthermore, the theory and method of analyzing thermoanalytical curves for the process of nucleation and growth described by Ozawa neglect the secondary crystallization that follows primary crystallization.

Hammami et al. [16] showed that Eq. (14) could be transformed into:

$$\theta(t) = 1 - \exp\left[-\Psi(T)t^n\right] \tag{15}$$

where t denotes the time required to cool the sample melt from the equilibrium melting temperature, T_m^0, to T. $\Psi(T)$ is the ratio of $K(T)$ to $(\Delta T)^n$. To express $\Psi(T)$, and hence $K(T)$, explicitly as a function of temperature, it is assumed that $\Psi(T)$ has the same temperature dependence as k and that the grown spherulites are three-dimensional. Using the Hoffman–Lauritzen theory for the growth rate of linear polymers with chain folds, $\Psi(T)$ is expressed as:

$$\Psi(T) = C_1 \exp\left[\frac{-3U^*}{\mathrm{R}(T - T_\infty)}\right] \exp\left[\frac{-3C_2}{fT\Delta T}\right] \tag{16}$$

where C_1 is a constant not strongly temperature dependent, and C_2 is a parameter related to the free energy of nucleation. This proposed model was successfully applied to experimental DSC data for three iPP resins with different molecular weights obtained at five cooling rates from 2 to 40°C/min.

In the study reported in this paper the majority of the models above will be re-examined to directly fit non-isothermal crystallization data for iPP obtained over a wide range of cooling rates from 1 to 100°C/min.

3. Experimental work

The grade of polypropylene (isotactic homopolymer) used in this study was FINA 4060S (containing no nucleating agent), with melt flow rate (MFI 230°C, 2.16 kg) = 3 g/10 min.

Isothermal and non-isothermal crystallization runs were carried out using a Perkin Elmer DSC7. Pure indium was used as a reference material to calibrate both the temperature scale and the melting enthalpy before the samples were tested. Sample weights of approximately 5.0 ± 0.1 mg were crimped in aluminum pans and loaded at 30°C to the DSC, heated up rapidly (40°C/min) to 200°C and maintained at this temperature for 3 min to remove thermal history. For isothermal crystallization, the melted samples were cooled down rapidly (100°C/min) to the required crystallization temperature and allowed to crystallize. Non-isothermal crystallization was carried out by cooling the melted samples down to 30°C at constant cooling rates of 1, 5,10, 30, 100°C/min.

To characterize the beginning of crystallization, the time corresponding to the intersection between the extrapolation of the DSC curves after crystallization and the same curve before crystallization has been selected. The relative crystallinity, which developed on cooling to temperature T, was defined as the fractional area confined between the rate time curve and the baseline on the measured DSC exotherm [2]. The temperatures were corrected for thermal lag between the samples and the calorimeter furnace using a calibration technique [17] employing pure indium.

Table 1
Tabulation of Avrami indices at different crystallization temperatures for iPP

T_c (°C)	Avrami index
120	3.56
125	3.37
128	3.18
130	2.82
133	3.12
135	2.92

The Levenburg and Marquardt [10] non-linear multivariable regression method was used to fit the non-isothermal crystallization data. The best values of N parameters are searched over a large region of N-dimensional space to find the global minimum in the sum of the square of errors.

4. Results and discussion

4.1. Isothermal crystallization

Relative crystallinities, $\theta(t)$, accumulated as a function of time for isothermal crystallization were calculated from the crystallization exotherms recorded via DSC. To obtain an idea of the mechanism of nucleation as well as the growth geometry, isothermal kinetics data have been analyzed using the logarithmic form of the Avrami equation (Eq. (2)). The Avrami analysis for iPP undergoing crystallization at different constant temperatures for relative crystallinities between 15 and 100% is shown in Fig. 1. The obtained values of Avrami indices (n), shown in Table 1, were found to be approximately 3 which suggests an instantaneous nucleation with spherical growth geometry. This is in keeping with the results of other researchers in this area: Hammami et al. [16] used Ozawa theory to analyze the isothermal crystallization kinetics for three different polypropylene resins and found that the spherulites were grown three-dimensionally with a heterogeneous nucleation. Hwang et al. [18] obtained values of n close to 3 for PET in its blends with poly(ether imide). Silvestre et al. [19] in their study found that for pure iPP, independent of the crystallization temperature, n always has a value of nearly 3. Srinivas et al. [20] reported an Avrami exponent of 3 for the phenyl sulfide polymers, independent of molecular weight or crystallization temperature. Hence, a value of 3 for n will be used in the subsequent non-isothermal crystallization kinetics analysis.

The Avrami plot exhibited a deviation from linearity at the later stages of crystallization. This deviation has been attributed to the occurrence of secondary crystallization [18].

4.2. Non-isothermal crystallization

To account for the thermal lag between a point in the sample and the calorimeter furnace, the recorded temperatures in non-isothermal experiments must be corrected [2,5,16,21]. In a previous study [22] it was found that the thermal lag is less than 1°C at low cooling rates (1, 5, 10°C/min), and about 9°C at the highest cooling rate (100°C/min) used in the study. All recorded non-isothermal crystallization data are corrected according to the following equation:

$$T_{\text{actual}} = T_{\text{disp}} + 0.089\lambda \tag{17}$$

where T_{disp} is the display temperature and λ(°C/min) is the cooling rate.

Relative crystallinities of non-isothermally crystallized iPP at various cooling rates are presented in Fig. 2. Using the literature values of 1500 cal/mol for U^* [2,5,16], 260 K for T_g [16], 460.7 K for T_m^0 [16], and keeping $n = 3$, different non-isothermal crystallization kinetics models were applied to directly fit (using the Marquardt's non-linear regression method) the non-isothermal crystallization data obtained in this work.

Fig. 3 shows a comparison between the experimental and predicted non-isothermal crystallinity data for iPP using the

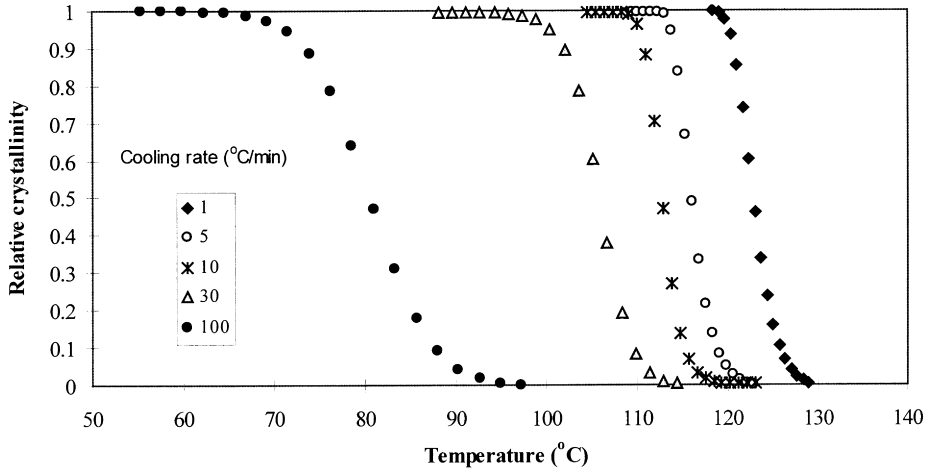

Fig. 2. Plot of relative crystallinity as a function of temperature for iPP (FINA 4060S) at different cooling rates.

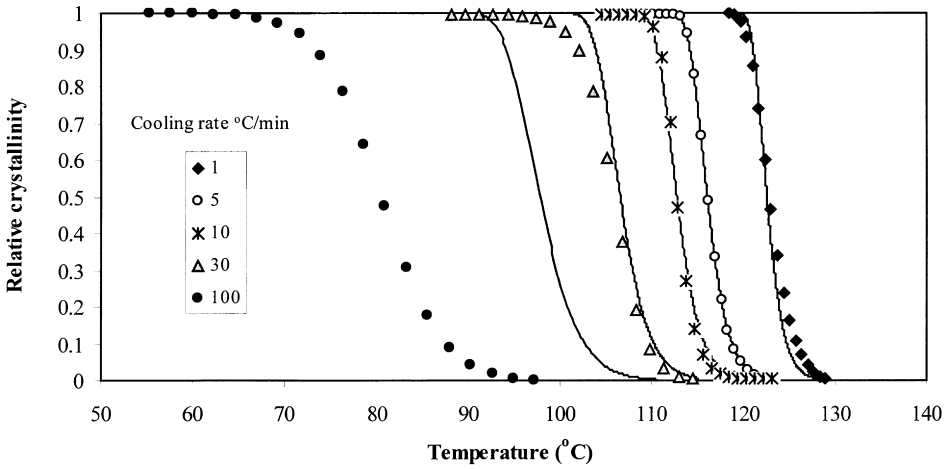

Fig. 3. Non-linear regression fitting of the non-isothermal crystallization data of iPP (FINA 4060S) using Kamal model (Eq. (4)). Solid lines are predicted data.

integral Kamal and Chu model (Eq. (4)) in conjunction with Eq. (7b), at different cooling rates. The integration was computed using $T_0 = T_m^0$ as a lower limit for the integration. It can be observed that the Kamal and Chu model overpredicts the non-isothermal crystallinity data especially at high cooling rate. This observation was made by Patel and Spruiell [2] when they re-examined the Kamal and Chu model (Eq. (4)) to predict non-isothermal crystallization from isothermal data for nylon 6. The authors found that the model overpredicts the non-isothermal crystallinity data over the cooling rates from 2 to 40°C/min. It was observed that predictions of non-isothermal crystallinity data using the Kamal and Chu model were very sensitive to the temperature from which one starts computing the integral. The appearance of the time as an explicit variable in the model, and the dependence of the value of the integral on when one starts counting residence time (t) which is very difficult to estimate, make the predictions very sensitive.

Predictions of non-isothermal crystallinity data using the integral Nakamura model (Eq. 3) in conjunction with Eq. (7b) at different cooling rates are presented in Fig. 4. Again the integration was computed using $T_0 = T_m^0$ as a lower limit for the integration. Predictions of the integral Nakamura model were not as sensitive to the variation of T_0 as the predictions of the Kamal and Chu model. The integral Nakamura model does not contain time as an explicit variable. It is clearly seen that the model predictions match the experimental data at very low cooling rate (1°C/min) only.

Fig. 5 compares the experimental and predicted non-isothermal crystallinity data using the differential Nakamura model for iPP at different cooling rates. To meet the numerical requirement of the model the initial crystallinity must be non-zero. A very small value of $\theta(0) = 10 \times 10^{-10}$ was assumed here. In comparison with Kamal and Chu and the integral Nakamura models, the differential Nakamura model gives better predictions but still does not match the experimental data at most cooling rates. Chen and Isayev [5] calculated the relative crystallinity developed during non-isothermal crystallization under various constant cooling/heating rates using the differential Nakamura model with

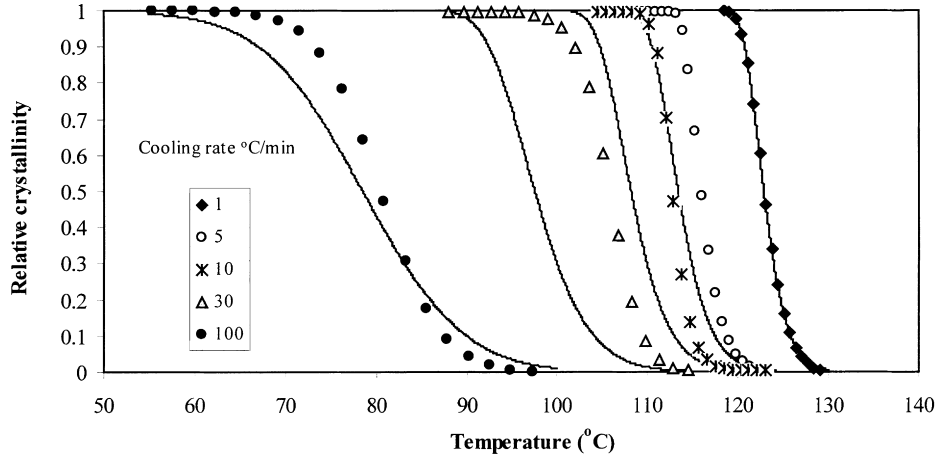

Fig. 4. Non-linear regression fitting of the non-isothermal crystallization data of iPP (FINA 4060S) using the integral Nakamura model (Eq. (3)). Solid lines are predicted data.

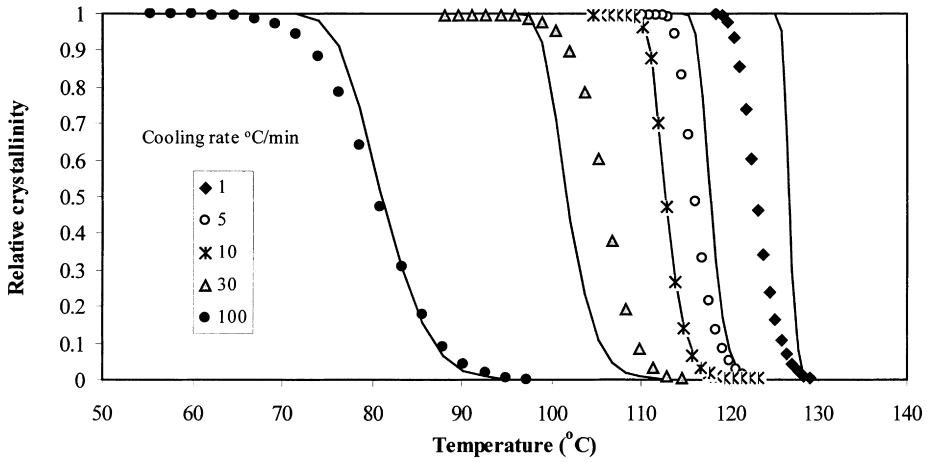

Fig. 5. Non-linear regression fitting of the non-isothermal crystallization data of iPP (FINA 4060S) using differential Nakamura model (Eq. (5)). Solid lines are predicted data.

$\theta(0) = 10 \times 10^{-15}$ as an initial condition. They found that without the incorporation of induction time, the model overpredicted the experimental results at most cooling/heating rates. Patel and Spruiell [2] reported that both the integral and differential forms of the Nakamura model (Eqs. (3) and (5)) overpredict the non-isothermal data mainly because the original Nakamura model (Eq. (3)) does not take into account the effect of induction time. To eliminate induction time effects, these authors used the lowest measurable crystallinity value obtained from the DSC at corresponding cooling rate as an initial condition in the differential form of the Nakamura model. However, the authors reported that both the integral and differential Nakamura models overpredict the non-isothermal data, with better predictions from the differential Nakamura model.

The next model examined was the simplified differential Nakamura model (Eq. (7)). As seen in Fig. 6, the predictions do not match the experimental data at high cooling rates. In general, the differential Nakamura models (Eqs. (5) and (7)) were found to be very sensitive to the assumed initial condition. Also, the isokinetic assumption, which is not likely to hold for large temperature changes and the spontaneous formation of nuclei are not taken into account in the model, making accurate predictions unlikely.

The modified non-isothermal crystallization model of Hammami and Mehrotra [16], Eq. (15) coupled with Eq. (16), was re-examined using Marquardt's non-linear regression to determine the kinetic parameters, C_1 and C_2, while keeping the Avrami index constant at $n = 3$. The predictions for non-isothermal crystallization are compared with the non-isothermal experimental data in Fig. 7. Predictions using this model match the experimental data only at low cooling rates. Hammami et al. [16] found $\ln(C_1)$ values ranging from 71.8 to 76.1 and C_2 values ranging from 5.5 to $5.9 \times 10^5 \mathrm{K}^2$, for cooling rates up to 40°C/min. These values are in good agreement with the values obtained in this work; $\ln(C_1) = 74.94$ and $C_2 = 5.87 \times 10^5 K^2$.

The next model examined was that of Velisaris and Seferis (Eq. (11b)). Keeping $n_1 = 3$ and $n_2 = 1$, the other five parameters of the model (C_1, C_2, C_3, C_4, and w_1) were

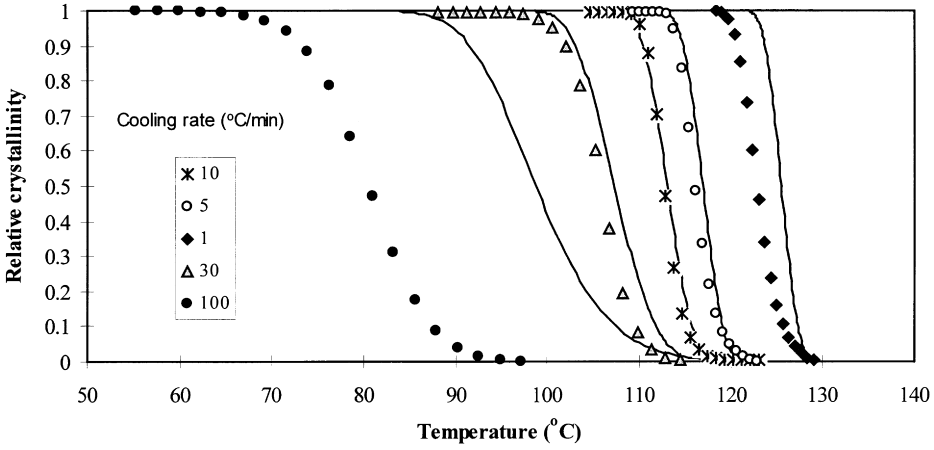

Fig. 6. Non-linear regression fitting of the non-isothermal crystallization data of iPP (FINA 4060S) using the simplified model (Eq. (15)). Solid lines are predicted data.

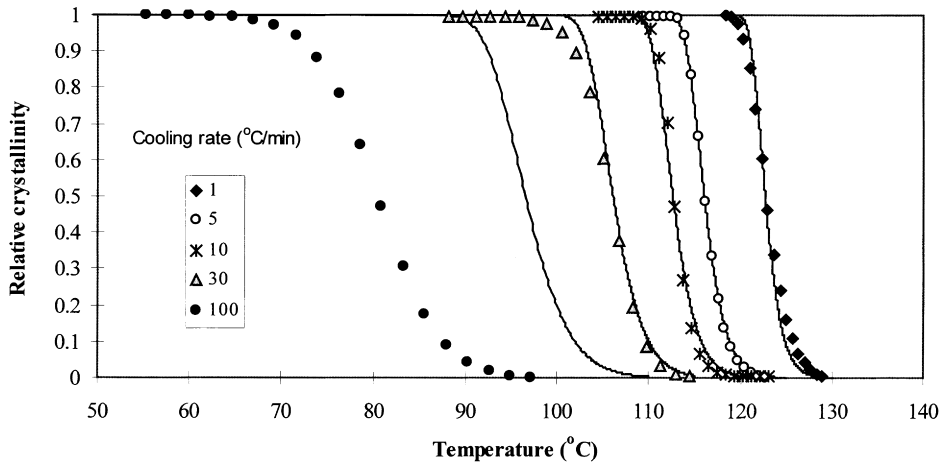

Fig. 7. Non-linear regression fitting of the non-isothermal crystallization data of iPP (FINA 4060S) using modified Ozawa model (Eq. (15)). Solid lines are predicted data.

allowed to vary and the best values to fit the data were obtained. (The same values for n_1 and n_2 were used by Woo and Yau [23] in a modified two stage model proposed to describe the crystallization from the melt state of a miscible binary blend system comprising amorphous poly(ether imide) and crystallizable poly(butylene terephthalate). Early stage crystallization exhibits a three-dimensional spherulite growth with heterogeneous nucleation, while crystal growth at later stage might most likely exhibit a fibral pattern in one-dimension. This was given as an explanation for these two different Avrami exponents.)

Fig. 8 shows a comparison between the predicted and experimental non-isothermal crystallization data for iPP at different cooling rates. In fact good correlation can be achieved with different sets of parameters for low cooling rates, while it was not possible to fit the experimental data at the highest cooling rate (100°C/min) using the same parameters (C_1, C_2, C_3, and C_4).

None of the models applied so far is adequate in predicting non-isothermal crystallization data over the full range of cooling rates (from 1 to 100°C/min). The proposed model by Hammami and Mehrotra (Eq. (15) coupled with Eq. (16)) has been shown to be the best of those reviewed. In all the re-examined non-isothermal crystallization models, the beginning of the crystallization process (equilibrium melting temperature in this study) was used as a reference time. However, between the beginning of a crystallization experiment and the emergence of the first crystalline nucleus, a certain period elapses which is called the induction time. It is necessary to include this effect in the model. Patel and Spruiell [2] have concluded that an overprediction of non-isothermal data can be attributed to the fact that traditional kinetic models do not account for this time.

Following the approach of Sifleet et al. [24], non-isothermal induction times can be obtained from isothermal

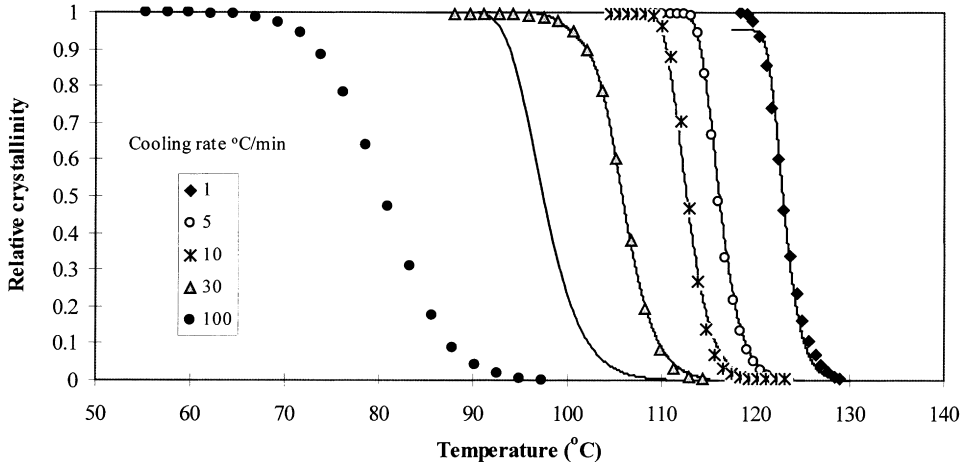

Fig. 8. Non-linear regression fitting of the non-isothermal crystallization data of iPP (FINA 4060S) using the parallel Avrami model (Eq. (11)). Solid lines are predicted data.

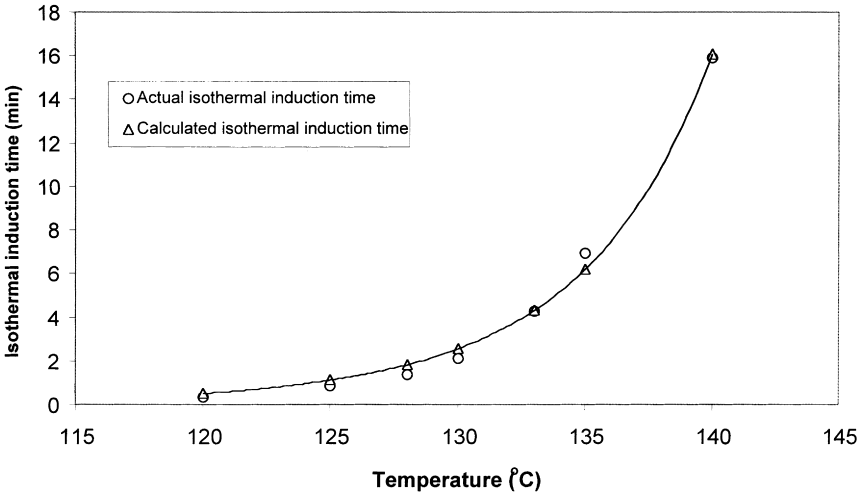

Fig. 9. Actual and calculated (Eq. (19)) isothermal induction times for iPP (FINA 4060S).

induction times according to:

$$\bar{t} = \int_0^{t_I} \frac{dt}{t_i(T)} = 1 \tag{18}$$

where $t_i(T)$ is the isothermal induction time as a function of temperature. When the value of the dimensionless induction time index $\bar{t}$ reaches unity, the upper limit of integration is taken as the non-isothermal induction time t_I.

The isothermal induction time t_i was obtained from isothermal DSC measurements, and is presented as a function of temperature in Fig. 9. For melt-crystallization, the following expression for t_i has been proposed [25]:

$$t_i = t_m(T_m - T)^{-a} \tag{19}$$

where t_m and a are material constants independent of temperature T, T_m is the temperature at which cooling of melted sample starts (= 200°C in the present work). Using non-linear regression fitting, $t_m = 3.0339 \times 10^{22}\text{min}/K^a$ and $a = 11.965$ were obtained. The agreement between actual and calculated isothermal induction times is presented in Fig. 9.

The non-isothermal induction time t_I was defined as:

$$t_I = \frac{T_m - T_s}{\lambda} \tag{20}$$

Table 2
Actual, calculated (Eq. (21b)) and estimated (Eq. (22b)) non-isothermal induction times for iPP (FINA 4060S)

Cooling rate (°C/min)	Actual induction time (min)	Calculated induction time (min)	Fitted induction time (min)
1	71	66.1	70.04
5	15.1	14.98	14.49
10	7.7	7.90	7.27
30	2.77	2.86	2.48
100	1.02	0.94	1.02

where T_s is the temperature at which the crystallization peak begins.

Using the same approach of Isayev et al. [26], the non-isothermal induction time (Eq. (18)) is simplified to:

$$\sum_0^{t_I} \frac{1}{t_m(T_m - T)^{-a}} \Delta t = 1 \tag{21a}$$

or

$$\sum_{T_0}^{T_s} \frac{1}{t_m(T_m - T)^{-a}} \frac{\Delta T}{\lambda} = 1 \tag{21b}$$

Using the isothermal model parameters (t_m and a), the non-isothermal induction time for any thermal history can be calculated. The results are given in Table 2.

Inclusion of the non-isothermal crystallization induction time in the proposed model by Hammami and Mehrotra (Eq. (15)) will yield:

$$\theta(t) = 1 - \exp\lfloor - \Psi(T)(t_0 - t_I)^n \rfloor \tag{22a}$$

or

$$\theta(t) = 1 - \exp\left[-\Psi(T)\left(\frac{T_s - T}{\lambda} \right)^n \right] \tag{22b}$$

where t_0 is the time required to cool the sample melt from T_m to T, T is the crystallization temperature, and t_I is the non-isothermal induction time.

Using the same values of U^*, T_g, T_m^0 and keeping $n = 3$, the same experimental non-isothermal data for iPP was fitted using the new proposed model (Eq. (22b) coupled with Eq. 16). This time three parameters were determined, C_1, C_2 and T_s. Fig. 10 shows that the predicted crystallization data matches the experimental data very well. The correlation coefficients, r^2, for the regression were ≥0.99. The obtained parameters $\ln(C_1) = 64.2$ and $C_2 = 4.5 \times 10^5 K^2$ vary from Hammami's values but this is expected for the wide range of cooling rates under

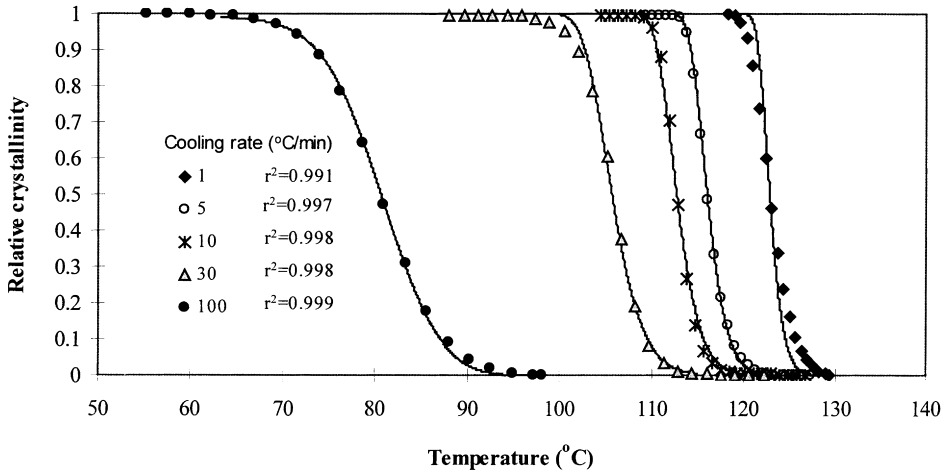

Fig. 10. Non-linear regression fitting of the non-isothermal crystallization data of iPP (FINA 4060S) using the modified model (Eq. (17)). Solid lines are the predicted data.

investigation. The proposed modification allowed excellent predictions of the non-isothermal data for iPP. Fig. 11 shows the predicted and the actual non-isothermal induction times. It can be seen that the predicted values are close to the real values.

By substitution of the determined parameters into Eq. 16 values of $\Psi(T)$ were calculated. It can be seen in Fig. 12 that PP exhibits a maximum crystallization rate at about 346 K. Magill [27] predicted a maximum crystallization rate which falls within the 333.2–343.2 K temperature range, and Hammami [16] reported a maximum crystallization rate at about 340.2 K.

5. Conclusions

Isothermal melt crystallization kinetics were analyzed using the logarithmic form of the Avrami equation. The value of the Avrami index obtained, $n = 3$, implies that the nucleation is instantaneous with spherical growth geometry.

In comparison with values from literature, good agreement for the kinetic parameters can be obtained using a non-linear regression method, particularly when the non-isothermal crystallization data obtained from the differential scanning calorimetry for iPP is corrected for the effect of temperature lag between the DSC sample and the furnace.

Based on the above study, it can be concluded that none of the non-isothermal crystallization kinetic models examined can quantitatively predict non-isothermal crystallization data without taking into account the effect of the induction time.

A modified Ozawa kinetic model taking into account the effect of the induction time is proposed to describe non-isothermal crystallization of iPP. Predictions using the modified model match the experimental data over the wide range of the cooling rates used in this study (from 1 to 100°C/min).

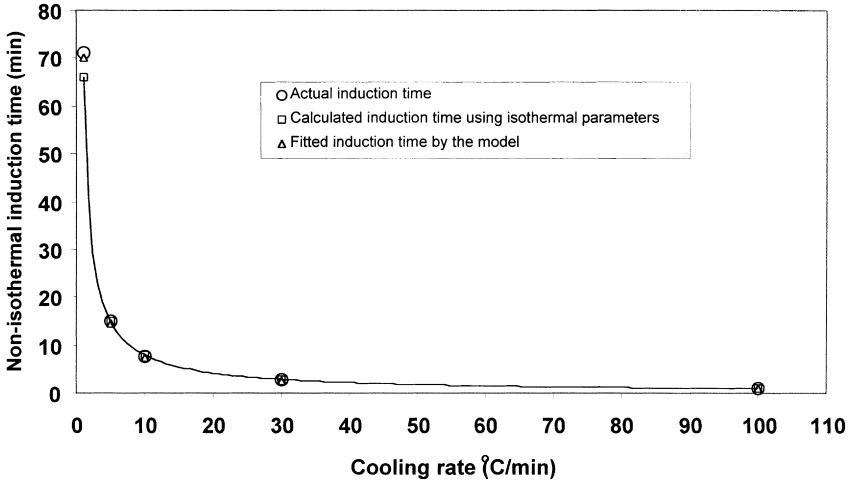

Fig. 11. Plot of non-isothermal induction times as a function of cooling rate for iPP (FINA 4060S).

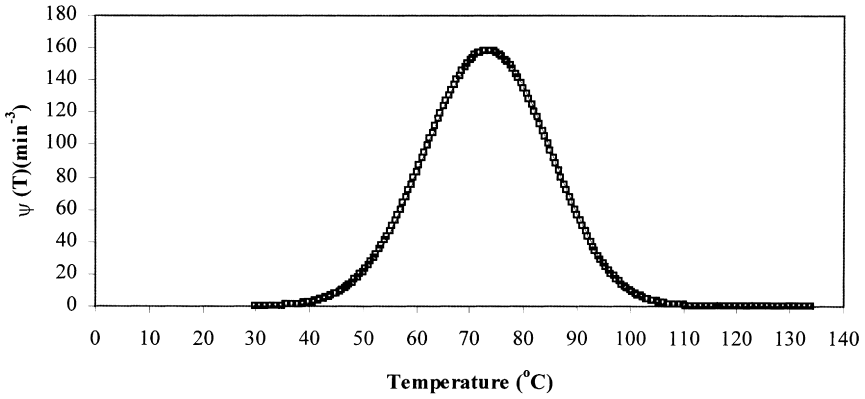

Fig. 12. Predicted temperature dependence of $\psi(T)$ for iPP (FINA 4060S).

References

[1] Avrami M. Journal of Chemical Physics 1940;8:221–4.
[2] Patel RM, Spruiell LJE. Polymer Engineering and Science 1991;31(10):730–8.
[3] Nakamura K, Katayama K, Amano T. Journal of Applied Polymer Science 1973;17:1031–41.
[4] Kamal MR, Chu E. Polymer Engineering and Science 1983;23:27–31.
[5] Chan TW, Isayev AI. Polymer Engineering and Science 1994;34(6):461–71.
[6] Dietz W. Colloid & Polymer Science 1981;259:413–29.
[7] Ding Z, Spruiell JE. Journal of Polymer Science, Part B: Polymer Physics 1997;35(7):1077–93.
[8] Kim YC, Kim CY, Kim SC. Polymer Engineering and Science 1991;31(14):1009–14.
[9] Choe CR, Lee KH. Polymer Engineering and Science 1989;29(12):801–5.
[10] Constantidinis A. Numerical methods with personal computers. New York: McGraw Hill, 1987.
[11] Hammami A, Mehrotra AK. Polymer Engineering and Science 1995;35(2):170–2.
[12] Velisaris C, Seferis J. Polymer Engineering and Science 1986;26(22):1574–81.
[13] Cebe P. Polymer Engineering and Science 1988;28(18):1192–7.
[14] Verhoyen O, Dupret F, Legras R. Polymer Engineering and Science 1998;38(9):1594–610.
[15] Ozawa T. Polymer 1971;12:150–8.
[16] Hammami A, Spruiell JE, Mehrotra AK. Polymer Engineering and Science 1995;35(10):797–804.
[17] Hammami A. Thermal Behavior And Non-Isothermal Crystallization Kinetics Of Normal-Alkanes and Their Waxy Mixtures Under Quiescent Conditions. PhD thesis, University of Calgary, Canada, 1994. p. 103–5.
[18] Hwang JC, Chen CC, Chen HL, Yang WO. Polymer 1997;38:4097–101.
[19] Silvestre C, Cimmino S, D'Alma E, Di Lorenzo ML, Di Pace E. Polymer 1999;40:5119–28.
[20] Srinivas S, Babu JR, Fiffel JS, Wilkes GL. Polymer Engineering and Science 1997;37:497–510.
[21] Monasse B, Haudin JM. Colloid & Polymer Science 1986;122:117–22.
[22] Mubarak Y, Harkin-Jones EMA, Martin PJ, Ahmad M. III Jordanian Chemical Engineering Conference, vol. I, 1999. p. 49–70.
[23] Woo EM, Yau SN. Polymer Engineering and Science 1998;38:583–9.
[24] Sifleet WL, Dinos N, Collier JR. Polymer Engineering and Science 1973;13:10.
[25] Godovsky YuK, Slonimsky GL. Journal of Polymer Science, Part B: Polymer Physics 1974;12:1053–80.
[26] Isayev AI, Chan TW, Shimojo K, Gmerek M. Journal of Applied Polymer Science 1995;55:807–19.
[27] Magill JH. Polymer 1962;3:35–42.